FOSL2 Directly Regulates FSHR and CYP11A1 Transcription: An Essential Transcription Factor for Gonadotropin-Dependent Folliculogenesis

Hongru Shi[1†], Chaoli Chen[2†], Zaohong Ran[1†], Jianning Liao[1], Zian Wu[1], Xiaodong Wang[1], Yongheng Zhao[1], Wenkai Ke[1], Bowen Tan[1], Yun Liu[1], Wei Ren[2*], Xiang Li[1*], Changjiu He[1*]

[1] Key Laboratory of Agricultural Animal Genetics, Breeding and Reproduction of Ministry of Education, College of Animal Sciences and Technology, Huazhong Agricultural University, Wuhan 430070, PR China;

[2] Department of Obstetrics, Maternal and Child Health Hospital of Hubei Province, Wuhan 430070, PR China;

[†] These authors contributed equally to this work.

***Corresponding Author**:

Wei Ren, Orcid ID: 0000-0002-1061-276X;

Email: 1393600775@qq.com; Maternal and Child Health Hospital of Hubei Province, Wuhan 430070, China.

Xiang Li, Orcid ID: 0000-0002-9168-1598;

Email: xxianglli@mail.hzau.edu.cn; Huazhong Agricultural University, Wuhan 430070, China.

Changjiu He, Orcid ID: 0000-0002-0350-9799;

Email: chungjoe@mail.hzau.edu.cn; Huazhong Agricultural University, Wuhan 430070, China.

Short title: Fosl2 functions on GTH-dependent folliculogenesis

ABSTRACT

Fosl2, a member of the AP-1 family, has been widely studied in the fields of tumorigenesis and immune response, but its role in folliculogenesis remains unclear. In this investigation, we presented comprehensive in vitro and in vivo evidence to precisely define the biological functions of Fosl2 in folliculogenesis. Fosl2 in both mouse and sheep, we demonstrated that the knockdown of *Fosl2* effectively inhibited cell proliferation and promoted cell apoptosis in both primary GCs and the GCs of cultured gonadotropin (GTH)-dependent follicles. To explore the in-vivo function of Fosl2, we generated an ovarian GC-specific conditional knockout (CKO) mouse model. CKO mice showed impaired GTH-dependent folliculogenesis, leading to disrupted estrous cycles and infertility in female mice. Subsequent bioinformatics analysis and experimental results indicated that Fosl2 regulates the transcription of FSHR and CYP11A1. These findings unveiled the essential role of Fosl2 in governing the development of GTH-dependent folliculogenesis, thereby providing a novel strategy for elucidating GTH-dependent folliculogenesis mechanisms and treating ovarian dysfunction.

Keywords: Fosl2, folliculogenesis, granulosa cell, estradiol, gonadotropin-dependent follicle

INTRODUCTION

Infertility has emerged as a significant global health concern, with impaired folliculogenesis representing a critical factor in female reproductive dysfunction[1]. Ovarian follicles, the fundamental functional units of ovary comprising oocytes and granulosa cells (GCs), serve as pivotal determinants of female fertility. GCs orchestrate folliculogenesis through multifaceted roles in oocyte-granulosa cell communication, metabolic regulation, hormonal synthesis, and signal transduction [2-6]. The granulosa cells are indispensable for oocyte maturation, GTH-dependent folliculogenesis (antrum formation and expansion), and post-ovulatory luteinization [7-9]. The GTH-dependent stage constitutes a decisive period governed by integrated endocrine networks involving gonadotropins, steroid hormones, growth factors, and inhibins, which collectively dictate follicular fate determination [10-13]. Elucidating regulatory mechanisms during this critical developmental period remains essential for advancing reproductive research.

Previous studies have reported numerous transcription factors that play key roles in the ovaries [14-16].Fos-like antigen 2 (Fosl2), a component of the transcription factor AP-1 family [17], modulates cellular processes including growth regulation, and immune responses [18-26]. It has been reported that homozygous mice with systemic knockout of Fosl2 died within one week after birth [27], and studies have also shown that abnormal expression of *Fosl2* can cause some diseases, such as asthma and pulmonary fibrosis[28, 29], suggesting that Fosl2 may play an important role in the regulation of animal organism. Although Fos family members regulate ovulation-related genes[30], and bioinformatic analyses implicate Fosl2 in polycystic ovary syndrome [31]. The specific reproductive functions of Fosl2 in folliculogenesis remain unknown.

This study demonstrates that *Fosl2* deficiency disrupts GTH-dependent folliculogenesis and induces female infertility. Transcriptome analysis revealed Fosl2 is highly expressed in ovarian granulosa cells and is induced by gonadotropin. GC-specific knockdown and conditional knockout impaired granulosa cell proliferation,

suppressed GTH-dependent folliculogenesis, and disrupted estrous cycle. Mechanistically, Fosl2 directly regulates the transcription of FSHR and CYP11A1 to exert its function. Our findings establish Fosl2 as an essential transcription factor of GTH-dependent folliculogenesis, providing new insights for improving the reproductive performance of humans and animals.

RESULTS

1. Characterization of the Fosl2

In order to further explore the transcription factors that play an important role in the development of follicles, we performed transcriptome analysis in mice ovarian granulosa cells from PMSG 0h to PMSG 24h [32]. The expression of the transcription factor Fosl2 was found to be significantly induced by PMSG (Figure 1A, B). The tissue expression profile of *Fosl2* in mice was mapped by qRT-PCR, confirming that Fosl2 was highly expressed in the ovary (Figure 1C). The results of qRT-PCR further confirmed that *Fosl2* expression was significantly induced by PMSG (Figure 1D.). Immunofluorescence staining confirmed that Fosl2 was mainly localized in GCs of ovarian follicles both in mouse and sheep (Figure 1E, F). These findings suggest that Fosl2 is mainly localized in ovarian GCs and induced by PMSG.

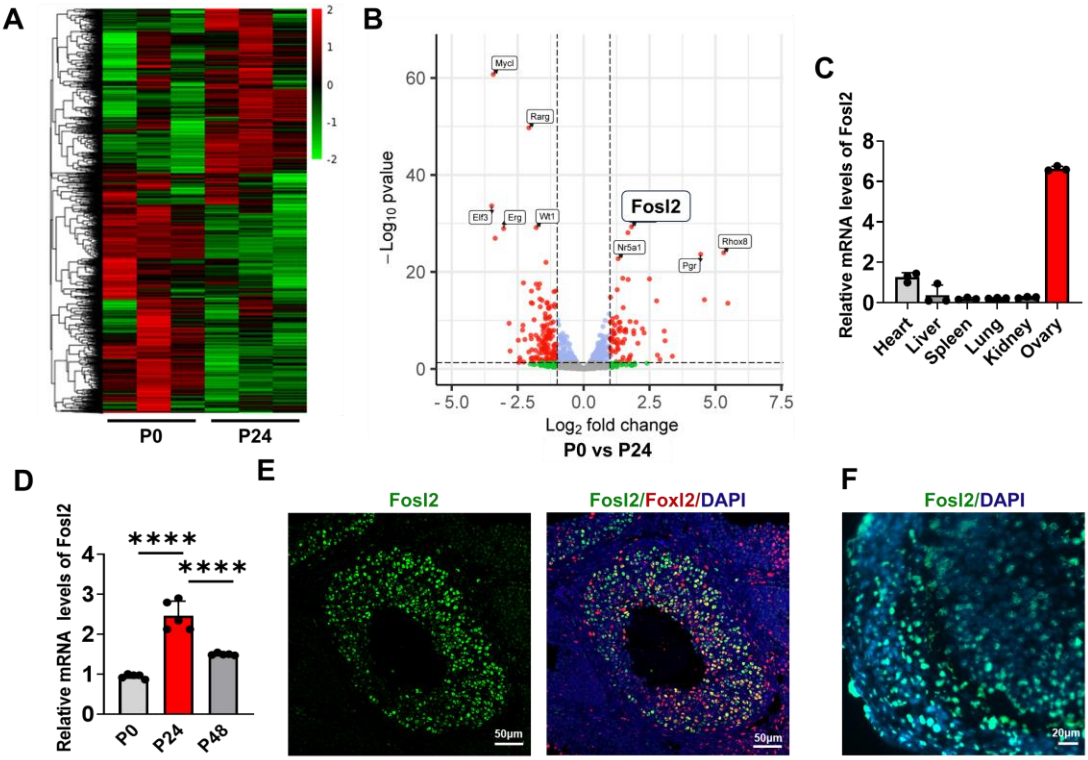

Figure 1. Fosl2 is highly expressed in ovarian GCs and induced by PMSG (A) Heatmap of the up-regulated genes in mGCs after PMSG injection. (B) Transcriptome analysis was used to identify the up-regulated and down-regulated genes of transcription factor in ovarian GCs after PMSG injection. Three GCs samples derived from six mice per group were used for RNA-seq. (C) Tissue expression profile of *Fosl2* gene in mice, n=3. (D) Expression of *Fosl2* gene in mouse ovarian GCs 0, 24, 48 hours after PMSG injection, n=5. (E) Immunofluorescence staining showed the localization of Fosl2 protein in follicles of mouse. Green is a positive stain for Fosl2 protein. Nuclear staining was performed with DAPI. (F) Immunofluorescence staining showed the localization of Fosl2 protein in follicles of sheep. Green is a positive stain for Fosl2 protein. Nuclear staining was performed with DAPI. Statistical significance were determined using one-way ANOVA followed by Tukey's post hoc test, values were mean ± SD. Significant differences were denoted by **P<0.01, ***P<0.005. The experiments were repeated independently two times, yielding consistent results.

2. Knockdown of *Fosl2* inhibits proliferation and promotes apoptosis in GCs

To investigate the function of Fosl2 in ovarian GCs, mouse primary GCs were isolated and transfected with siRNA targeting *Fosl2*, with knockdown efficiency confirmed (Figure 2A, B). Flow cytometric analysis of cell cycle distribution revealed that *Fosl2*-knockdown significantly increased the proportion of cells in G1 phase while reducing populations in S and G2 phases (Figure 2C), indicating G1 phase arrest and impaired DNA synthesis. Real-time cell analysis (RTCA) showed delayed entry into the rapid proliferation phase and reduced cell index peak in *Fosl2*-knockdown GCs (Figure 2D). EdU staining further demonstrated suppressed proliferation in *Fosl2*-knockdown cells (Figure 2E).

Then the apoptosis of *Fosl2*-knockdown GCs was detected. Flow cytometry analysis showed that knockdown of *Fosl2* resulted in a significant increase in the proportion of annexin-V-positive cells, indicating an increase in GCs at an early apoptotic stage (Figure 2F). Knockdown of *Fosl2* significantly increased the expression of the apoptosis marker protein Cleaved-Caspase3 (Figure 2G). Further TUNEL staining showed that the proportion of apoptotic cells was significantly increased (Figure 2H). Sheep primary GCs were isolated and transfected with siRNA targeting *Fosl2* (Figure 2I, J). Similarly, apoptosis of cells is enhanced (Figure 2K, L). Conversely, *Fosl2* overexpression (Figure S1A) reduced the proportion of early apoptotic cells (Figure S1B), confirming the regulatory role of Fosl2 in apoptosis.

These results demonstrate that *Fosl2* knockdown inhibits proliferation and promotes apoptosis in ovarian GCs.

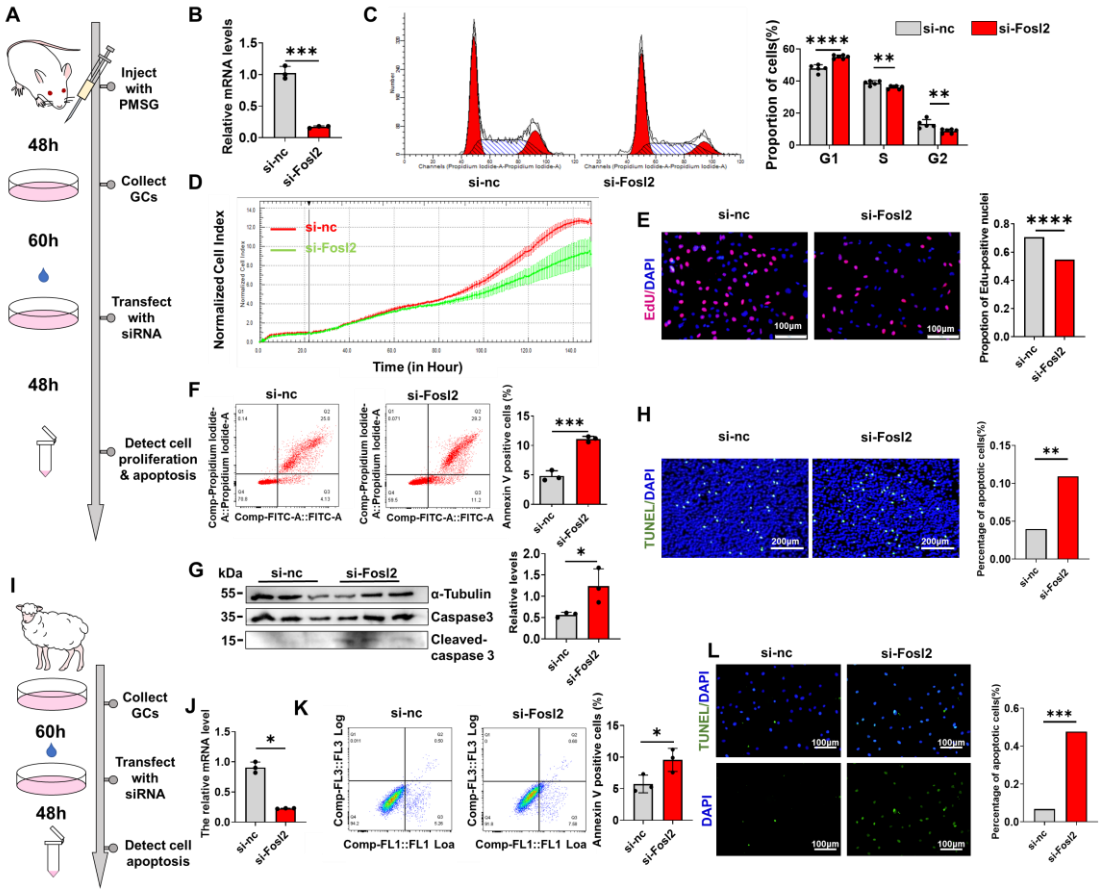

Figure 2. *Fosl2* knockdown on GCs inhibits cell proliferation and promotes apoptosis. (A-I) Knockdown Fosl2 in GCs of mouse. (A)Schematic representation of the knockdown or overexpress of *Fosl2* in primary mouse GCs. (B) Efficiency analysis of *Fosl2* interference using qRT-PCR, n=3. The scrambled siRNA was used as *si-nc* in this study. (C) Effect of *Fosl2*-knockdown on cell cycle, left: Representative images of cell cycle by flow cytometry, right: Cell cycle distribution, n=5(*si-nc*), 6(*si-Fosl2*). (D) Effect of *Fosl2*-knockdown on rapid cell proliferation. (E) EdU staining of Fosl2-knockdown cells, with red dots representing newly divided cells, left: Representative fluorescence images of EdU staining, right: Cell proliferation rate. (F) Flow cytometry results of apoptosis after *Fosl2*-knockdown, left: representative images of apoptosis detected by flow cytometry, right: Proportion of Annexin-V positive cells, n=3. (G) Western blot assay of apoptosis related protein contents of *Fosl2*-knockdown primary GCs, left: Expression of apoptosis-related proteins, right: Mean gray values, n=3. Original blots can be viewed in Figure S4A. (H) TUNEL staining of *Fosl2*-knockdown cells, green represents apoptosis-positive cells, left: Representative fluorescence images of TUNEL staining, right: Cell apoptosis rate. (I-L) Knockdown Fosl2 in GCs of sheep. (I) Schematic representation of the knockdown or overexpress of *Fosl2* in primary GCs. (J) Efficiency analysis of *Fosl2* interference using qRT-PCR, n=3. (K) Flow cytometry results of apoptosis after Fosl2-knockdown, left: representative images of apoptosis detected by flow cytometry, right: Proportion of Annexin-V positive cells, n=3. (L) TUNEL staining of *Fosl2*-knockdown cells, green represents apoptosis-positive cells, left: Representative fluorescence images of TUNEL staining, right: Cell

apoptosis rate. Statistical significance was determined using two-tailed unpaired Student's t test or chi-square test, values were mean ± SD. Significant differences were denoted by*P<0.05, **P<0.01 ***P<0.005, ****P<0.001. The experiments were repeated independently two times, yielding consistent results.

3. Knockdown of *Fosl2* impairs gonadotropin-dependent folliculogenesis

To investigate the direct effects of Fosl2 on folliculogenesis, we employed a previously established *in vitro* follicle culture system of mouse [33] and sheep. The expression of *Fosl2* was disrupted by lentivirus transfection of shRNA in follicles at different developmental stages.

Firstly, *Fosl2* was knocked down in the pre-antral (GTH-independent) follicles of mouse (Figure 3A), and observed fluorescence at 48 h after transfection (Figure 3B). After the completed transfection, the follicles were transferred to fresh maturation medium and cultured for 48h. The samples were collected after the follicular cavity can be clearly observed. The interference efficiency was verified by protein levels (Figure 3B). There was no significant difference in follicle volume and cavity area index (Figure 3C). EdU staining of antral follicle sections further demonstrated no significant difference (Figure 3D). Together, these data suggest that interfering with *Fosl2* in secondary follicles has no significant effect on their development.

Subsequent investigations focused on small antral (GTH-dependent) follicles. The antral follicles were transfected and collected (Figure 3E, F). Measurements revealed significant reductions in follicle volume and cavity area index, indicating restraint of antral cavity expansion in *Fosl2*-knockdown follicles (Figure 3G). EdU staining of follicular sections demonstrated suppressed granulosa cell proliferation (Figure 3H). qRT-PCR analysis further showed downregulation of proliferation-related genes (*PCNA*, *Ki67*, *Cyclin E1*; Figure S2). These findings conclusively demonstrate that *Fosl2*-knockdown impairs GTH-dependent folliculogenesis by suppressing antral expansion and granulosa cell proliferation.

Moving on to sheep, Fosl2 was knockdown in antral follicles (Fig 3I, J). Similarly, the volume of Fosl2-knockdown follicles was significantly reduced (Fig 3K).

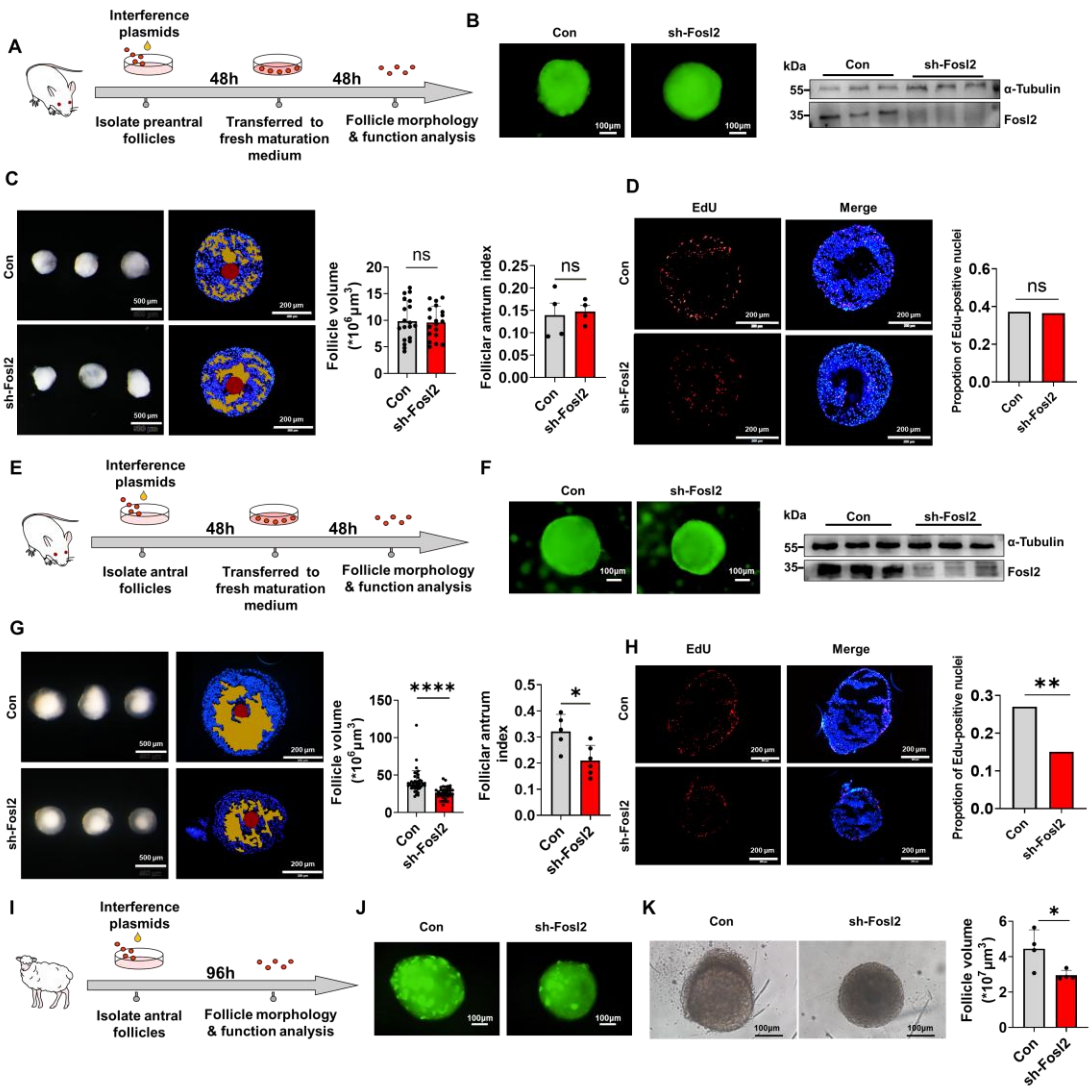

Figure 3. Effect of *Fosl2* knockdown on folliculogenesis at different stages. (A-D) *Fosl2* was knocked down in the cultured GTH-independent follicles in vitro. (A) Schematic representation of the knockdown of *Fosl2* in cultured GTH-independent follicles. (B) Efficiency analysis of *Fosl2* interference, left: Green fluorescence indicates successful transcription of interfering plasmids in follicles, right: Western blot assay of protein contents of Fosl2, n=3. Original blots can be viewed in Figure S4B. The scrambled shRNA was used as *Control* in this study. (C) Changes in the GTH-independent follicle volume, n=19 and follicular antrum index, n=4. (D) EdU staining of GTH-independent follicles, left: Representative fluorescence images of EdU staining, right: Cell proliferation rate, n=4. (E-H) *Fosl2* was knocked down in the cultured GTH-dependent follicles in vitro. (E) Schematic representation of the knockdown of *Fosl2* in cultured GTH-dependent follicles. (F) Efficiency analysis of Fosl2 interference, left: Green fluorescence indicates successful transcription of interfering plasmids in follicles, right: Western blot assay of protein contents of Fosl2, n=3. Original blots can be viewed in Figure S4C. (G) Changes in the GTH-dependent follicle volume, n=42 follicles (Con), 37 follicles (sh-Fosl2) and follicular antrum index, n=5 follicles (Con), 6 follicles (sh-Fosl2). (H) EdU staining of GTH-dependent follicles, left: Representative

fluorescence images of EdU staining, right: Cell proliferation rate, n=7 follicles (Con), 6 follicles (sh-Fosl2). (I-K) *Fosl2* was knocked down in the cultured GTH-dependent follicles of sheep in vitro. (I) Schematic representation of the knockdown of *Fosl2* in cultured GTH-dependent follicles of sheep. (J) Green fluorescence indicates successful transcription of interfering plasmids in follicles. (K) Changes in the GTH-dependent follicle volume, n=4. Statistical significance was determined using two-tailed unpaired Student's t test or chi-square test, values were mean ± SD. Significant differences were denoted by*P<0.05, **P<0.01 ****P<0.001. The experiments were repeated independently two times, yielding consistent results.

4. Conditional knockout of *Fosl2* in GCs leads to arrested GTH-folliculogenesis in female mice

In order to further explore the effect of Fosl2 on GTH-dependent folliculogenesis at individual level, we constructed a GCs-specific *Fosl2* knockout mouse model (*CKO*). We crossed *Fosl2*$^{flox/flox}$ with *FSHR-Cre* mice to create a *GCs-Cre; Fosl2*$^{fl/fl}$ mouse (Figure 4A). Immunofluorescence staining and WB were utilized to verify the knockout efficiency (Figure 4B, C).

An obvious estrus cycle disorder can be observed in adult female *CKO-Fosl2* mice of three estrus cycles (Figure 4D). Subsequent fertility assessments demonstrated significantly reduced mating rates in *CKO* mice compared to *Fosl2*$^{flox/flox}$ mice, with only one successful mating and no pregnancy (Figure 4E), indicating *Fosl2* conditional knockout induced female infertility. The serum estradiol content of mice also decreased (Figure 4F). Since the estrous cycle is closely related to folliculogenesis, we counted the ovarian weight of *CKO-Fosl2* mice and found that the ovarian weight decreased significantly after the conditional knockout (Figure 4G), suggesting that there may be abnormal folliculogenesis. HE staining of the ovarian sections at PMSG 48 h revealed a significant reduction in the number of preovulatory follicles (Figure 4H), which indicated that the arrested folliculogenesis led to the infertility of the mice. The molecular phenotypes of ovarian GCs in CKO mice were also examined (Figure S3). These findings collectively demonstrate that *Fosl2* knockout impedes GTH-dependent folliculogenesis, ultimately leading to female infertility.

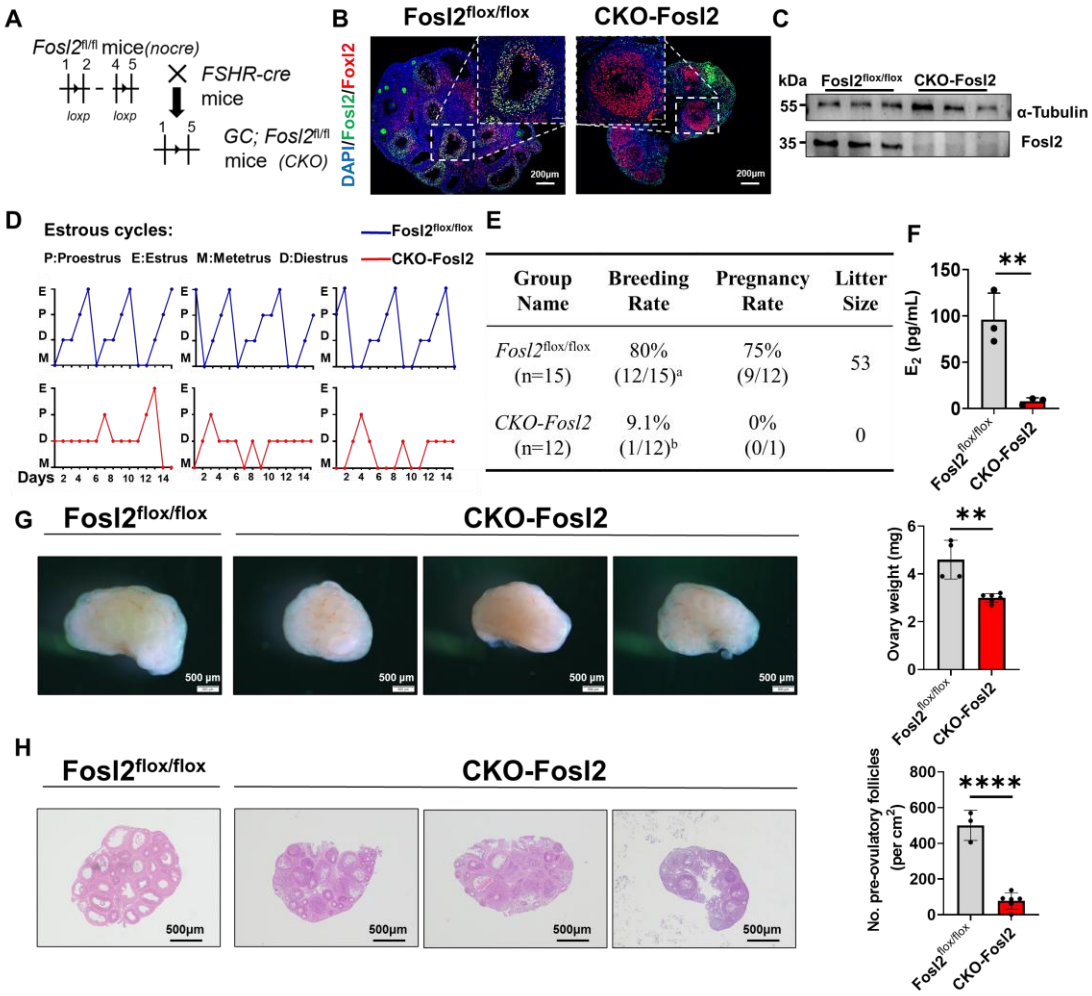

Figure 4. Fosl2 conditional knockout result in infertility in female mice. (A) Schematic representation of the Fosl2 conditional knockout in GCs of mice. Exon 2-4 deletion via *FSHR-Cre*-mediated recombination in GCs within *GC; Fosl2$^{flox/flox}$* (*CKO*). (B) Immunostaining showed that the *Fosl2* gene was successfully knocked out in ovarian GCs of CKO mice, blue: DAPI, green: Fosl2, red: Foxl2. (C) Western blot assay of protein contents of *CKO-Fosl2* mice, n=3. Original blots can be viewed in Figure S4D. (D) Representative plot of estrous cycles, n=10. (E) Breeding rate, pregnancy rates, litter size of *CKO-Fosl2* mice. (F) Effect of conditional knockout of ovarian GCs on estradiol levels in serum, n=3 serum samples. (G) Morphological analysis of ovary after 48 hours of PMSG treatment, left: Representative photographs, right: Statistical graph, n=4 ovaries (*Fosl2$^{flox/flox}$*), 6 ovaries (*CKO-Fosl2*). (H) H&E staining of ovaries 48 h after PMSG treatment, left: Representative photographs, right: Follicle number statistics, n=3 ovaries (*Fosl2$^{flox/flox}$*), 6 ovaries (*CKO-Fosl2*). Statistical significance was determined using two-tailed unpaired Student's t test, values were mean ± SD. Significant differences were denoted by **P<0.01 ****P<0.001. The experiments were repeated independently two times, yielding consistent results.

5. Fosl2 regulates FSHR and CYP11A1 transcription

To elucidate the mechanism of Fosl2 in GTH-dependent folliculogenesis, we used JASPAR and FIMO databases to predict the potential binding sites of Fosl2 protein to key genes in folliculogenesis. Analysis showed that *Fosl2* may target genes that play a core role in GTH-dependent folliculogenesis (Figure 5A). The EMSA result revealed FOSL2 binding to the *Fshr* promoter and *Cyp11a1* promoter (Figure 5B).

To validate the aforementioned hypothesis, we examined the expression levels of *FSHR* and *CYP11A1* in *Fosl2*-knockdown GCs using qRT-PCR. The results demonstrated that *Fosl2*-knockdown significantly downregulated the mRNA expression (Figure 5C). Further, qRT-PCR analysis of Fosl2-knockdown cultured follicle model indicated the similar results (Figure 5D). Consistent results were observed in GCs of *CKO* mice (Figure 5E).

These results suggest that FOSL2 can bind to critical genes' promoter such as *Fshr* and *Cyp11a1*.

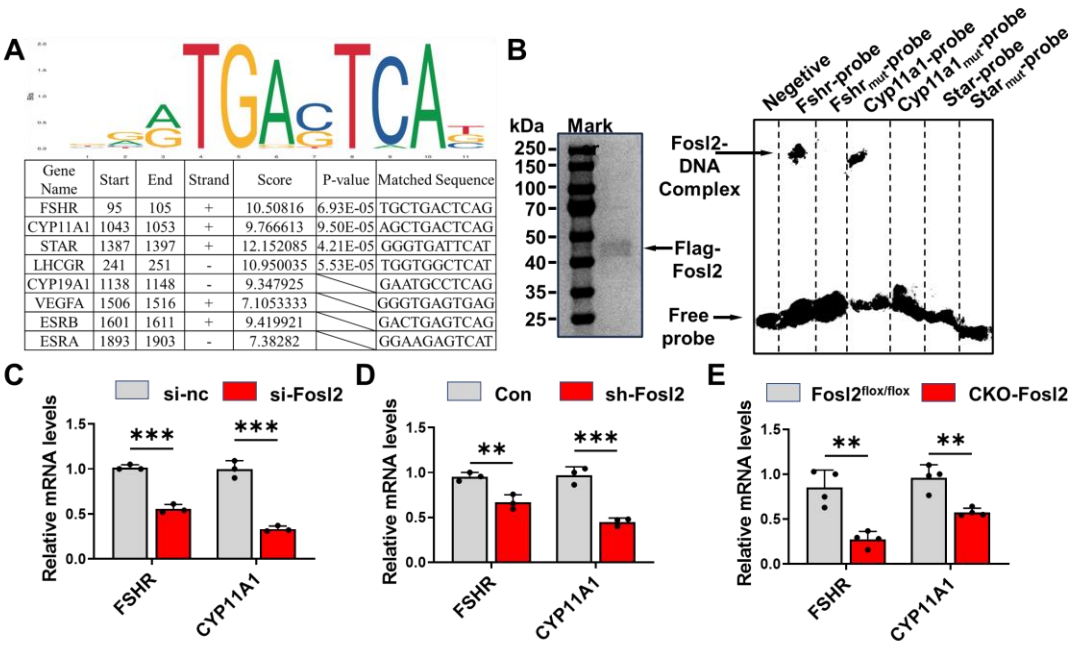

Gene Name	Start	End	Strand	Score	P-value	Matched Sequence
FSHR	95	105	+	10.50816	6.93E-05	TGCTGACTCAG
CYP11A1	1043	1053	+	9.766613	9.50E-05	AGCTGACTCAG
STAR	1387	1397	+	12.152085	4.21E-05	GGGTGATTCAT
LHCGR	241	251	-	10.950035	5.53E-05	TGGTGGCTCAT
CYP19A1	1138	1148	-	9.347925		GAATGCCTCAG
VEGFA	1506	1516	+	7.1053333		GGGTGAGTGAG
ESRB	1601	1611	+	9.419921		GACTGAGTCAG
ESRA	1893	1903	-	7.38282		GGAAGAGTCAT

Figure 5. FOSL2 directly bind to the promoter of *Fshr* and *Cyp11a1*. (A) Prediction of possible binding sites of *Fosl2* and GTH-dependent folliculogenesis genes. (B) EMSA demonstrated FOSL2 binding to *Fshr* and *Cyp11a1* promoter sequences. (C) Expression of genes of *FSHR* and *CYP11A1* of GCs in F*osl2*-knockdown primary GCs, n=3. (D) Expression of genes of *FSHR* and *CYP11A1* of GCs after *Fosl2* knockdown in cultured follicles, n=3. (E) Expression of genes of *FSHR* and *CYP11A1* in GCs of *CKO* mice, n=4. Statistical significance was determined using two-tailed unpaired Student's t test, values were mean ± SD. Significant differences were denoted by*P<0.05, **P<0.01, ***P<0.005, ****P<0.001. The experiments were repeated independently two times, yielding consistent results.

DISCUSSION

As a transcription factor affecting a variety of cells, Fosl2 is highly expressed in ovarian GCs, but its effect on folliculogenesis remains underexplored. In this study, we investigated the effects of Fosl2 on GTH-dependent follicles in vitro and in vivo. Fosl2 knockdown leads to proliferation arrest and apoptosis of primary GCs and GTH-dependent follicles. Notably, we demonstrate that granulosa cell-specific *Fosl2* knockout causes female infertility in mice.

In previous studies, Fosl2 has been shown to be expressed and function in a variety of cells and tissues. Including mediating renal tubular epithelial cell transdifferentiation in fibrosis [34], suppressing myogenic differentiation in porcine muscle stem cells[35], driving senescence in hepatic progenitor-like cells [36], negatively regulating NK cell development [37]. The function of GCs is closely related to folliculogenesis and maturation. Our identification of Fosl2's ovarian enrichment and PMSG-induced expression suggests its critical involvement in folliculogenesis (Figure 1). Further studies showed that Fosl2 knockout had no significant effect on the growth of GTH-independent follicles, but only affected the GTH-dependent follicles (Figure 3). This suggests that knockdown of *Fosl2* inhibits folliculogenesis by inhibiting granulosa cell proliferation and GTH-dependent follicle antral expansion. This is also consistent with the effect of Fosl2 on inhibiting proliferation in other cells.

Since Fosl2 is stably expressed during the early development of animals and total deletion leads to lethality, the conditional knockout method can be adopted for the research on Fosl2 in specific tissues. Smith et al. have constructed conditional knockout rats of *Fosl2* in the pineal gland [38], and Chen et al. have constructed conditional knockout mice with hematopoietic system deficiency [39]. In this study, after conditional knockout of *Fosl2* in mouse ovarian GCs, the mice showed disorders of estrus cycles and infertility. The mating rate of CKO mice was extremely low, and they did not become pregnant even after successful mating. The morphological analysis of the ovaries suggested that the knockout of Fosl2 was accompanied by a decrease in

preovulatory follicles, which was consistent with its inhibitory effect on the growth of GTH-dependent follicles (Figure 4).

Bioinformatics analysis and experimental verification indicated that Fosl2 can regulate the expression of genes related to estradiol synthesis (Figure 5). This finding is consistent with the conclusion that members of the AP-1 family are involved in the transcription regulation of steroid synthetase [40]. At the same time, the expression of genes related to granulosa cell differentiation *FSHR*, also significantly decreased while the expression of genes related to estradiol synthesis *CYP11A1*, significantly decreased. The direct regulation of *FSHR* and *CYP11A1* by Fosl2 suggests that this regulation has an important influence on some signaling pathways downstream of folliculogenesis [41, 42].

At present, this study still has limitations. For future studies, we will further explore the signaling pathways that Fosl2 regulate when it plays the role of regulating folliculogenesis, and explore the expression and role of Fosl2 in males. In addition, the role of Fosl2 in the regulation of folliculogenesis in sheep remains to be further studied. The materials and methods employed in this study will be described in detail in the final submission version.

In conclusion, this study demonstrates that FOSL2 directly regulates FSHR and CYP11A1 transcription as an essential transcription factor for gonadotropin-dependent folliculogenesis. Moreover, conditional knockout of *Fosl2* in GCs of follicles leads to disrupted estrous cycles and infertility in female mice. These findings elucidate the important role of Fosl2 in the folliculogenesis process and fertility in female mice. This study supplements the regulatory mechanism of GTH-dependent folliculogenesis and provides a new approach for improving folliculogenesis, as well as new insights for enhancing the fertility of female animals and humans.

MATERIALS AND METHODS

Animals

Kunming mice were purchased from the Center for Animal Testing of Huazhong Agricultural University (Wuhan, China). *Fosl2*$^{flox/flox}$ C57BL/6J mice were purchased from GemPharmatech Co., Ltd., and FSHR-Cre mice were donated by Prof. Su (Shandong University, China). Mice were reared in an SPF laboratory animal house, at a constant temperature of 22±2℃, being allowed to access food and water ad libitum with 12h light-dark cycles. Sheep samples are collected from slaughterhouses. All experiments and handling of animals were approved and guided by the Institutional Animal Ethics Committee of Huazhong Agricultural University Committee.

Construction of *Fosl2* ovarian granulosa cell conditional knockout mouse model: The exon2-exon4 of the Fosl2-201 (ENSMUST00000031017.10) transcript was used as the knockout region. Ex vivo transcription of sgRNA was carried out to construct the donor vector. Cas9, sgRNA and the targeting vector were injected into the fertilized eggs of C57BL/6J mice through microinjection technology. F0 generation positive mice were obtained by transplantation of fertilized eggs and verified by PCR and sequencing. The F0 positive mice were crossed with C57BL/6J mice to obtain stable F1 generation flox heterozygous mice models. F1 generation mice were mated with each other to obtain *Fosl2*$^{flox/flox}$ mice. *Fosl2*$^{flox/flox}$ mice were crossed with FSHR-Cre mice to obtain the conditional knockout heterozygotic mice of Fosl2 in granulosa cells (*Fosl2*$^{+/-Cre}$). *Fosl2*$^{+/-Cre}$ mice were crossed with *Fosl2*$^{flox/flox}$ mice to obtain the conditional knockout mice of *Fosl2* in granulosa cells, *Fosl2*$^{flox/flox\ Cre}$ (*CKO-Fosl2*).

Superovulation

Mice were injected 5IU pregnant mare serum gonadotropin (PMSG) (Ningbo Sansheng Biological Technology) to promote follicle growth. 48 hours after injection of PMSG, 5IU human chorionic gonadotropin (hCG) (Ningbo Sansheng Biological Technology) was injected to promote ovulation.

Analysis of RNA-seq

The mouse transcriptome data were sequenced in-house, with granulosa cells isolated

from pre-ovulatory follicles at 0- and 24-hours post PMSG injection. Specific transcriptome sequencing method was described in previous research [32].

Analysis of qRT-PCR

Total RNA from samples was extracted using TRIzol reagent (Takara, 9109, Japan) and cDNA was obtained by reverse transcription using Evo M-MLV RT Kit (AGbio, AG11728, China). qRT-PCR was performed by CFX384 Real-Time PCR System (Bio-Rad). Reaction system includes: SYBR Green (Biosharp, China), 2 μL complementary DNA template, 250 nM of the forward and reverse primers for each, and ddH_2O was supplemented to a total volume of 10 μL. The reaction protocol was conducted as described: an initial denaturation step at 95 ℃ for 10 min, succeeded by 35 cycles comprising denaturation at 95 ℃ for 10 s and annealing/ extension at 60°C for 30 s. Using ACTB to normalize gene expression levels, and using comparative $2^{-\triangle\triangle Ct}$ method to determine relative RNA quantification. The primer sequences are provided in Table S1.

Western Blot

Extract total protein with lysis buffer consist of RIPA (ComWin Biotech, China), protease and phosphatase inhibitors (ComWin Biotech, China) and PMSF (Solarbio, China). Protein content was measured using BCA Protein Assay Kit (Servicebio, China). Protein bands were separated sufficiently by SDS polyacrylamide gel electrophoresis (SDS-PAGE) and transferred onto a polyvinylidene fluoride membrane. After blocking the band with 5% skim milk powder (Nestle) at room temperature, incubated the band overnight at 4℃ with the primary antibodies. Primary antibodies listed as follows: Fosl2 (1:1000, Abclonal), α-Tubulin (1:1000, Biodragon-immunotech), Caspase3 (1:1000, Cell Signaling Technology), Cleaved-Caspase3 (1:1000, Abclonal), Bax (1:1000, Cell Signaling Technology). Next, rinsed the bands with TBST (Servicebio, China) and incubated with the secondary antibody: goat anti-rabbit immunoglobulin G (1:4000, Biodragon-immunotech, China), goat anti-mouse immunoglobulin G (1:4000, Biodragon-immunotech, China) for 120 min at room temperature. After rinsing with TBST, the bands were visualized with ECL chemiluminescent reagent kit (Servicebio, China) and acquire photographs with the Chemiluminescence Imager (Image Quant LAS 4000 mini, USA). The housekeeping protein α-tubulin was used for gray value

statistic normalize.

Immunofluorescence Staining

The collected ovaries were embedded in 4% paraformaldehyde (Servicebio, China) to be immobilized. After paraffin embedding, the ovaries were sliced into sections of 5 μm. Following dewaxing and antigen retrieval, the samples were treated with 0.5% Triton-X-100 in PBS for 15 min to facilitate permeabilization, followed by blocking with 5% donkey serum for 30 min. Subsequently, the sections were incubated with the FOSL2 (1:100, Abclonal)/FOXL2 (1:100, Abclonal) antibody at 4℃ overnight. After rinsing, the sections were incubated with the goat anti-rabbit immunoglobulin G (1: 10000, Biodragon-immunotech, China) at 37℃ for 60 min. Cell nuclei were stained with DAPI at room temperature for 5 min. Next, the samples were rinsed and subsequently sealed with an anti-fluorescence quencher. Images were taken using the LSM800 confocal microscope system (Zeiss, Germany).

Culture of primary granulosa cells

Primary granulosa cells were collected after puncturing mouse or sheep ovarian follicles, filtered and inoculated into culture dishes. Cells were cultured at 37 ℃ in a 5% CO_2 incubator using 10% fetal bovine serum (FBS) (Serana, Germany), DMEM/ F12 (Gibco, Carlsbad, CA, USA) with 1% penicillin-streptomycin (Servicebio, China). Subculturing after 48 h for subsequent experiments.

Culture of follicles

Mouse: The follicles of different sizes were isolated from mouse ovaries using 33-gauge microneedles (KONSFI, China) for the experiment of follicles at different stages. The size of Small preantral follicles is 100-120 μm, and the size of antral follicles is 180-200 μm. Isolated follicles were cultured in 96-well plates (BKMAM, China), covered with mineral oil (Sigma, Germany), and in an incubator maintained at 37 ℃ and 5% CO_2. The main components of follicle maturation medium include：α-MEM (Gibco, USA), 5% FBS (Serana, Germany), 1% ITS (Macklin, China), 100 U/mL penicillin–streptomycin (Servicebio, China) and 10 mIU/mL FSH (NSHF, China).

Sheep: The follicles of different sizes were isolated from sheep ovaries using ophthalmic scissors and 26-gauge microneedles (KONSFI, China) for the experiment

of follicles at different stages. Isolated follicles were cultured in 96-well plates (BKMAM, China), covered with mineral oil (Sigma, Germany), and in an incubator maintained at 38.5 °C and 5% CO_2. The main components of follicle maturation medium include：α-MEM (Gibco, USA), 10% FBS (Serana, Germany), 1% ITS (Macklin, China), 100 U/mL penicillin–streptomycin (Servicebio, China),50 μg/mL ascorbic acid, 2 mM hypoxanthine, 2 mM glutamine and 10 mIU/mL FSH (NSHF, China).

RNA Interference and Overexpression

Using si-RNA to inhibit the expression of target genes in Cells: When reached about 50% confluence, cells were transfected with siRNA using jetPRIME transfection reagent. 48h later, cell samples were collected or conducted further experiments.

Lentivirus-mediated RNA interference was used to inhibit the expression of target genes in follicles. Briefly, PLKO.1-EGFP-PURO plasmid (Genecreate, China) was utilized to construct interference vectors. Small interfering RNA targeted Fosl2 sequence is 5’- ATCATTGACCGCTCCTTTAGGT-3’. Negative siRNA, pMD2.G and pSPAX were purchased from Genecreate. Lentiviruses were produced in 293 T cells (ATCC, USA) by co-transfecting 4.8 μg interference vector, 2.4 μg pMD2.G, and 3.6 μg pSPAX2. The viral supernatants were harvested after 48 h, centrifuged, and filtered through 0.45 μm polyvinylidene fluoride membranes (Sigma, USA). Follicles with a specific diameter (mouse: around 140 μm, sheep: around 300 μm) were selected for GTH-independent follicle knockdown Fosl2, and follicles with a diameter of around 180 μm were selected for GTH-dependent follicle knockdown Fosl2 to ensure that Fosl2 was knocked down before follicular antrum formation. Follicles were cultured in medium with 10 μg/mL polybrene and 100 μL/mL viral supernatants (mouse: 48h, sheep: 96h). The medium was replaced with normal maturation medium after the green fluorescence of the follicles was observed.

Using plasmid to overexpression the target genes in Cells: The protein coding region of mouse Fosl2 gene (CCDS: CCDS19190.1, length 981bp) was inserted into the BamHI XhoI cloning site of pcDNA 3.1 plasmid to construct an overexpression vector. Transfection was completed using jetPRIME transfection reagent.

Flow Cytometry

Cell cycle: Primary granulosa cells transfected 48 h be collected and resuspended with 500 μL cold 70% ethanol at 4 ℃ overnight. After rinsing with PBS, the cell samples were incubated with Rnase/PI at room temperature for 60 min. Early apoptosis: Primary granulosa cells transfected 48 h be collected and resuspended with Annexin V-FITC binding buffer. Add Annexin V-FITC/PI and incubate at RT for 15 min. Cell cycle and apoptotic cells were estimated in a flow cytometer (Beckman Coulter).

Real-time Cell Analysis

The cellular dynamic proliferation was monitored using the RTCA DP Instrument (Roche, Switzerland) based on electronic impedance detection. Cells were seeded in E-plate16 at an adjusted density of 7×10^4 cells/mL. Subsequently, 100 μL of cell suspension was dispensed into each well of the E-plate16. Following a 30-minute incubation at room temperature to facilitate cell sedimentation, the E-plate16 was transferred to the RTCA station for continuous impedance monitoring. The proportion of impedance change was continuously recorded, which was expressed by cell index, with data acquisition performed at 30-minute intervals over a 160-hour observation period. Cellular transfection was implemented at the 14th hour post-monitoring initiation.

EdU Staining

Use EdU assay kit (Ribo Bio, China) to measure cell proliferation in cells and follicles. Primary granulosa cells: 100 μL 50 μmol/L EdU be supplemented into the interfered cells, and the cells were immobilized after 2h incubation. Follicles: 50 μL 1 mg/kg EdU be supplemented into the interfered follicles, after incubating 24 h, used OCT (Sakura, USA) embed the follicles and frozen, and employed Cryostat (Leica, Germany) to section the follicle into 5 μm slices. Cell slides and follicle sections were incubated with 1× Apollo staining solution for 30 min. The nuclei were stained with 1× Hoechst33342 reaction solution for 30 min. After staining and rinsing, images were collected using a fluorescence microscope (Olympus, Japan).

TUNEL Staining

Cellular sample preparation method: The primary granulosa cell slides with interfering factors were fixed with 4% paraformaldehyde (Servicebio, China) for 15 min, then

rinsed with PBS. Subsequently, 0.2% TritonX-100 in PBS was added and incubated at 37°C for 10 min. After rinsing with PBS, 100 μL of TdT Equilibration Buffer was added to each sample and incubated at 37°C for 10-30 min. The TdT Equilibration Buffer was then removed and the labeling working solution was added. Incubation was carried out at 37°C in the dark for 60 min. After rinsing, DAPI was added and incubated for 5 min. The samples were then sealed with an anti-fluorescence quencher.

The preparation method for frozen sections of follicles was the same as that for EdU staining. Frozen sections were fixed with 4% paraformaldehyde (Servicebio, China) for 30 min, rinsed with PBS, and then 5 μg/mL proteinase K working solution was added to each sample and incubated at 37°C for 10 min. The subsequent steps were the same as those for cell slide staining. After staining, images were captured using a fluorescence microscope (Olympus, Japan). Normal nuclei are shown in blue and apoptotic cells in green. Apoptosis rate was the proportion of apoptotic cells to total cell number.

H&E Staining

Vaginal smear staining: The dried vaginal smears were dyed with hematoxylin and eosin respectively for 60 s, then fully rinsed and dried, and observed under a microscope. Ovary section staining: Ovarian tissue sections were deparaffinized and rehydrated and stained with hematoxylin for 6min, eosin for 20s. Then dehydrated with various concentrations of alcohol and removed with xylene. Stained sections were sealed with neutral gum, and images were obtained using a microscope (Olympus, Japan) for analysis.

Estrus cycle determination and mating

Vaginal smears of sexually mature mice aged 8 weeks were collected daily for H&E staining and the stage of estrus was examined for 15 days (3 estrus cycles). The mice that were confirmed to be in estrus were mated with male mice at night, and the vaginal plugs were checked the next morning to ensure whether the mating was successful.

Prediction of binding sites

JASPAR (https://jaspar.genereg.net/) and FIMO (https://meme-suite.org/meme/tool-s/fimo) were utilized to predict the binding sites of Fosl2 protein and gonadotropin, focusing on follicle-related genes.

Electrophoretic mobility shift assay (EMSA)

The FOSL2 Coding sequence was cloned into the pcDNA3.1-3XFlag plasmid (Addgene, China) for overexpression. Flag-tagged FOSL2 proteins were immunoprecipitated using an anti-Flag antibody (Beyotime, P2271, China). The elution of proteins from the antibody was carried out with elution buffer (0.1 M glycine, pH 2.7) and then neutralized using a neutralization buffer (1 M Tris, pH 8.5). Biotin-labeled DNA probes obtained from Genecreate (China) were utilized for the DNA EMSA, conducted with the Chemiluminescent EMSA Kit (Beyotime, GS009, China), following the manufacturer's instructions. In brief, recombinant Flag-FOSL2 and biotin-labeled DNA probes were incubated in binding buffer for 30 minutes at room temperature before being separated on a 4% native polyacrylamide gel at 100 V in TBE buffer (Beyotime, R0223, China). Subsequently, the DNA-protein complexes were transferred onto Amersham Hybond-N^+ membranes (Cytiva, RPN1510B, USA), blotted with HRP-conjugated streptavidin, and visualized via autoradiography.

Hormone Determination

Estradiol in serum was detected by radioimmunoassay kit (the Bioengineering Institute China). Sera were obtained by centrifuging whole blood at 3000 rpm for 10 min. Detection kit was purchased from the Bioengineering Institute (Nanjing, China) and commissioned the North Institute of Biological Technology (China) for testing.

Statistics Analysis

Statistical analyses were using GraphPad Prism 10.0 (GraphPad). Data were expressed as the mean ± SD. Two-tailed unpaired Student’s t test and one-way analysis of variance followed by Tukey’s post hoc test were used to analyze the statistical significance between two groups and among multiple groups, respectively. Chi-squared test was used in the comparison between the percentages. The statistical significance was set at P-value <0.05.

DATA AVAILABILITY

All data are available from the corresponding author upon reasonable request.

FUNDING

This research was supported by the Fundamental Research Funds for the Central Universities (2662023DKPY001) and the National Natural Science Foundation of China (31701301).

SUPPORTING INFORMATION

This article contains supporting information.

ACKNOWLEDGEMENTS

We are grateful to Prof. Yongqiang Su (Shandong University, China) and Prof. Dr. Louis Dubeau (University of South California, USA) for providing the FSHR-Cre mice.

AUTHORS' CONTRIBUTION

C.H. conceived, designed, conducted the experiments, analyzed and interpreted the data; H.S., C.C. and Z.R. anticipated in experiment design and conduction, data analysis, and manuscript preparation; J.L., Z.W., X.W., Y.Z., W.K., B.T. and Y.L. assisted with sample collection and experiments conduction; C.H., H.S., W.R. C.C. and Z.R. wrote the manuscript; X.L. and W. R. improved the manuscript. C.H., X.L., W.R. supervised and funded this project. All authors approved the final version.

DECLARATION OF INTERESTS

The authors declare that they have no conflicts of interest with the contents of this article.

REFERENCES

1. Njagi, P., et al., *Financial costs of assisted reproductive technology for patients in low- and middle-income countries: a systematic review.* Human Reproduction Open, 2023. **2023**(2).
2. Racowsky, C. and R.A. Satterlie, *Metabolic, fluorescent dye and electrical coupling between hamster oocytes and cumulus cells during meiotic maturation in vivo and in vitro.* Dev Biol, 1985. **108**(1): p. 191-202.
3. Sutton-McDowall, M.L., R.B. Gilchrist, and J.G. Thompson, *The pivotal role of glucose metabolism in determining oocyte developmental competence.* Reproduction, 2010. **139**(4): p. 685-95.
4. Pelland, A.M., H.E. Corbett, and J.M. Baltz, *Amino Acid transport mechanisms in mouse oocytes during growth and meiotic maturation.* Biol Reprod, 2009. **81**(6): p. 1041-54.
5. Chen, Y., S. Wang, and C. Zhang, *The Differentiation Fate of Granulosa Cells and the Regulatory Mechanism in Ovary.* Reprod Sci, 2024.
6. Richards, J.S. and S.A. Pangas, *The ovary: basic biology and clinical implications.* J Clin Invest, 2010. **120**(4): p. 963-72.
7. Liu, W., et al., *Transcriptome Dynamics and Cell Dialogs Between Oocytes and Granulosa Cells in Mouse Follicle Development.* Genomics Proteomics Bioinformatics, 2024. **22**(2).
8. Bosdou, J.K., et al., *Association of Basal Serum Androgen Concentration with Follicles Number on the Day of Triggering Final Oocyte Maturation in Low Responders According to the Bologna Criteria: A Prospective Cohort Study.* Int J Mol Sci, 2025. **26**(4).
9. Wang, X., et al., *Granulosa Cell-Layer Stiffening Prevents Escape of Mural Granulosa Cells from the Post-Ovulatory Follicle.* Adv Sci (Weinh), 2024. **11**(33): p. e2403640.
10. Knox, R.V., *Follicle development in pigs: State of the art.* Mol Reprod Dev, 2023. **90**(7): p. 480-490.
11. Nilsson, E.E., C. Detzel, and M.K. Skinner, *Platelet-derived growth factor modulates the primordial to primary follicle transition.* Reproduction, 2006. **131**(6): p. 1007-15.
12. Liu, X.M., et al., *Mitochondrial Function Regulated by Mitoguardin-1/2 Is Crucial for Ovarian Endocrine Functions and Ovulation.* Endocrinology, 2017. **158**(11): p. 3988-3999.
13. Knight, P.G., L. Satchell, and C. Glister, *Intra-ovarian roles of activins and inhibins.* Mol Cell Endocrinol, 2012. **359**(1-2): p. 53-65.
14. Nishigaki, A., et al., *HIF-1α Promotes Luteinization via NDRG1 Induction in the Human Ovary.* Biomedicines, 2025. **13**(2).
15. Knapp, E.M., et al., *Nuclear receptor Ftz-f1 promotes follicle maturation and ovulation partly via bHLH/PAS transcription factor Sim.* Elife, 2020. **9**.
16. Castrillon, D.H., et al., *Suppression of ovarian follicle activation in mice by the transcription factor Foxo3a.* Science, 2003. **301**(5630): p. 215-8.

17. Renoux, F., et al., *The AP1 Transcription Factor Fosl2 Promotes Systemic Autoimmunity and Inflammation by Repressing Treg Development.* Cell Rep, 2020. **31**(13): p. 107826.
18. Li, S., et al., *Fos-like antigen 2 (FOSL2) promotes metastasis in colon cancer.* Exp Cell Res, 2018. **373**(1-2): p. 57-61.
19. Wu, L., et al., *Natural Coevolution of Tumor and Immunoenvironment in Glioblastoma.* Cancer Discov, 2022. **12**(12): p. 2820-2837.
20. Zheng, S. and Y. Liu, *Progress in the Study of Fra-2 in Respiratory Diseases.* Int J Mol Sci, 2024. **25**(13).
21. Chen, D., et al., *TXNDC9 promotes hepatocellular carcinoma progression by positive regulation of MYC-mediated transcriptional network.* Cell Death Dis, 2018. **9**(11): p. 1110.
22. Stellato, M., et al., *The AP-1 transcription factor Fosl-2 drives cardiac fibrosis and arrhythmias under immunofibrotic conditions.* Commun Biol, 2023. **6**(1): p. 161.
23. Rampioni Vinciguerra, G.L., et al., *Role of Fra-2 in cancer.* Cell Death Differ, 2024. **31**(2): p. 136-149.
24. He, J., et al., *miR-597 inhibits breast cancer cell proliferation, migration and invasion through FOSL2.* Oncol Rep, 2017. **37**(5): p. 2672-2678.
25. Sun, X., et al., *miR-143-3p inhibits the proliferation, migration and invasion in osteosarcoma by targeting FOSL2.* Sci Rep, 2018. **8**(1): p. 606.
26. Hu, Y., et al., *LncRNA GSTM3TV2 Promotes Cell Proliferation and Invasion via miR-597/FOSL2 Axis in Hepatocellular Carcinoma.* Biomed Res Int, 2021. **2021**: p. 3445970.
27. Eferl, R., et al., *Development of pulmonary fibrosis through a pathway involving the transcription factor Fra-2/AP-1.* Proc Natl Acad Sci U S A, 2008. **105**(30): p. 10525-30.
28. Birnhuber, A., et al., *Transcription factor Fra-2 and its emerging role in matrix deposition, proliferation and inflammation in chronic lung diseases.* Cell Signal, 2019. **64**: p. 109408.
29. Ucero, A.C., et al., *Fra-2-expressing macrophages promote lung fibrosis in mice.* J Clin Invest, 2019. **129**(8): p. 3293-3309.
30. Zou, L., et al., *Bioinformatics analysis of the common targets of miR-223-3p, miR-122-5p, and miR-93-5p in polycystic ovarian syndrome.* Front Genet, 2023. **14**: p. 1097706.
31. Southall, J., et al., *Granulosa cell expression of Fos is critical for regulating ovulatory gene expressions in the mouse ovary.* Faseb j, 2025. **39**(4): p. e70388.
32. Chen, Y., et al., *A mouse model reveals the events and underlying regulatory signals during the gonadotrophin-dependent phase of follicle development.* Molecular Human Reproduction, 2020. **26**(12): p. 920-937.
33. Wang, X., et al., *The FSH-mTOR-CNP signaling axis initiates follicular antrum formation by regulating tight junction, ion pumps, and aquaporins.* J Biol Chem, 2023. **299**(8): p. 105015.

34. Liu, N., et al., *FOSL2 participates in renal fibrosis via SGK1-mediated epithelial-mesenchymal transition of proximal tubular epithelial cells.* J Transl Int Med, 2023. **11**(3): p. 294-308.
35. Zhou, P., et al., *Identification of novel transcription factors regulated by H3K27 acetylation in myogenic differentiation of porcine skeletal muscle satellite cells.* Faseb j, 2024. **38**(21): p. e70144.
36. Ding, M., et al., *Integration of ATAC-Seq and RNA-Seq reveals FOSL2 drives human liver progenitor-like cell aging by regulating inflammatory factors.* BMC Genomics, 2023. **24**(1): p. 260.
37. Schnoegl, D., et al., *Fra-2 Is a Dominant Negative Regulator of Natural Killer Cell Development.* Front Immunol, 2022. **13**: p. 909270.
38. Smith, M., et al., *Tissue-specific transgenic knockdown of Fos-related antigen 2 (Fra-2) expression mediated by dominant negative Fra-2.* Mol Cell Biol, 2001. **21**(11): p. 3704-13.
39. Chen, J., et al., *Fosl2 Deficiency Predisposes Mice to Osteopetrosis, Leading to Bone Marrow Failure.* The Journal of Immunology, 2024. **212**(7): p. 1081-1093.
40. Nguyen, H.T., M. Najih, and L.J. Martin, *The AP-1 family of transcription factors are important regulators of gene expression within Leydig cells.* Endocrine, 2021. **74**(3): p. 498-507.
41. Cai, J., et al., *Poor ovarian response to gonadotropin stimulation is associated with low expression of follicle-stimulating hormone receptor in granulosa cells.* Fertil Steril, 2007. **87**(6): p. 1350-6.
42. Li, Y., et al., *LHCGR and ALMS1 defects likely cooperate in the development of polycystic ovary syndrome indicated by double-mutant mice.* Journal of Genetics and Genomics, 2021. **48**(5): p. 384-395.